European Review for Medical and Pharmacological Sciences 2019; 23: 10204-10210

Downregulation of miR-21 promotes tibial fracture healing in rabbits through activating ERK pathway

J. SHENG, W.-D. LIANG, C.-H. XUN, T. XU, J. ZHANG, W.-B. SHENG

Department of Spine Surgery, the First Affiliated Hospital of Xinjiang Medical University, Urumqi, Xinjiang Uyghur Autonomous Region, China

Jun Sheng and Weidong Liang contributed equally to this work

Abstract. – OBJECTIVE: The aim of this study was to investigate the effect of micro ribonucleic acid (miR)-21 on tibial fracture healing in rabbits by regulating the extracellular signal-regulated kinase (ERK) signaling pathway, and to explore its possible underlying mechanism.

MATERIALS AND METHODS: A total of 15 healthy male rabbits were randomly divided into three groups, including: model group A (fracture group, n=5), model group B (fracture treatment group, n=5), and model group C (miR-21 siRNA + treatment group, n=5). Fracture healing was observed by imaging. The content of the serum collagen I and collagen II in rabbits was detected *via* enzyme-linked immunosorbent assay (ELISA). The morphology of bone tissues was observed *via* staining. Moreover, the expressions of ERK, transforming growth factor-β1 (TGF-β1), and Smad in osteoblasts of tibia were observed *via* Western blotting and Reverse Transcription-Polymerase Chain Reaction (RT-PCR), respectively.

RESULTS: There was bony callus formation in group B and C when compared with group A. Compared with group B, bony callus formation was significantly accelerated in group C, while healing cycle was shortened. Hematoxylin-eosin (HE) staining and Masson staining indicated that compared with group A, group C had more fibrous calluses, new capillaries, and fibroblasts in tissues. Meanwhile, group C exerted better maturity of collagen tissues and higher osteoid content at 20 d after modeling. Compared with group C, there were more osteoid tissues with poor maturity in group B. Meanwhile, intramembranous bone formation was deformed, and collagen content was remarkably lower in group B. The content of serum collagen I and collagen II remarkably increased in group B compared with group A ($p<0.05$). However, it was significantly upregulated in group C compared with group B, showing statistically significant differences ($p<0.05$). According to the results of Western blotting, the protein expressions of TGF-β1, Smad, and ERK in osteoblasts were significantly upregulated in group B when compared with those in group A ($p<0.05$). However, they increased remarkably in group C when compared with group B ($p<0.05$). Besides, RT-PCR results revealed that the messenger RNA (mRNA) expressions of TGF-β1, Smad, and ERK in osteoblasts were significantly higher in group B than those in group A ($p<0.05$). However, they were markedly raised in group C in comparison with group B ($p<0.05$).

CONCLUSIONS: Down-regulation of miR-21 promotes tibial fracture healing in rabbits by activating the ERK signaling pathway.

Key Words:
MiR-21, ERK, TGF-β1, Fracture, Bone healing.

Introduction

Fracture, as a common disease in clinical medicine, directly or indirectly leads to rupture of some parts of the bone. Original bone morphology can be restored through treatment. However, the deformities can also be caused in bone morphology if there is no timely treatment. This may ultimately make fracture healing difficult. Therefore, fracture healing is a very complex process of tissue changes[1]. Promoting bone healing and inhibiting bone resorption play leading roles in cell growth and development, as well as the composition of extracellular matrix[2]. The recovery process of bone fracture, disintegration, and injury mostly belong to the healing of bone tissues. From the perspective of physiological histology [hematoxylin-eosin (HE) staining and Masson staining], this mainly includes the inflammatory stage, callus stage, and osteogenesis stage. In the inflammatory stage, the main manifestations are hematoma and production of inflammatory cells. In the callus stage, scabs appear on the primary bones. Meanwhile, there are fibrocytes and new capillaries. In the osteogenesis

Corresponding Author: Weibin Sheng, MD; e-mail: wbsheng@vip.sina.com

stage, bone lamella takes shape, which usually lasts for 1-2 years[3,4]. All these findings indicate that bone healing is a long physiological process. Among the reasons that can affect this series of changes, the growth factors are dominated[5]. Previous studies have found that transforming the growth factor-β1 (TGF-β1), can exert multiple biological effects through transformation, including inhibiting tissue apoptosis, accelerating cell differentiation, increasing collagen content, and reducing bone loss[6].

Micro ribonucleic acids (miRNAs) are a kind of endogenous small-molecule single-stranded RNAs. They have been found widely involved in bone healing, which can directly or indirectly promote the growth, development, and apoptosis of osteoblasts. MiR-21, as a member of miRNAs, also possesses the same physiological functions[7]. Extracellular signal-regulated kinase (ERK) is an extracellular regulatory protease that can convey cytokines by signaling pathway. Ultimately, this can alter the development of cell growth factors. Targeting the regulatory protease and activating the signaling pathway can directly or indirectly regulate cell proliferation and apoptosis[8,9]. Currently, the correlations of TGF-β1 with ERK signal and miR-21 remain unclear[10]. In this paper, therefore, the rabbit model of fracture was first established. The effect of miR-21 on tibial fracture healing in rabbits was analyzed by regulating the ERK signaling pathway. Our findings might help to provide a basis for the treatment of fractures in the future.

Materials and Methods

Experimental Reagents

Reverse transcription kit was purchased from Thermo Fisher Scientific (Waltham, MA, USA), trypsin, and medium from HyClone (South Logan, UT, USA), polyvinylidene difluoride (PVDF) membrane from Selleck (Houston, TX, USA), Dulbecco's Modified Eagle's Medium (DMEM) containing fetal bovine serum (FBS) from Sangon (Shanghai, China), high-speed centrifuge from Sigma-Aldrich (Louis, MO, USA), and 37°C incubator from Shanghai Fuma Laboratory Instrument Co., Ltd. (Shanghai, China).

Experimental Grouping

A total of 15 healthy male adult rabbits weighing (3 ± 0.3) kg were enrolled in this study (purchased from Hunan SJA Laboratory Animal Co., Ltd., Hunan, China). All rabbits were randomly divided into three groups, including: group A (fracture group without treatment, n=5), group B (penicillin sodium treatment group, n=5), and group C [injection of miR-21 small interfering RNA (siRNA), n=5]. This investigation was approved by the Animal Ethics Committee of Xinjiang Medical University Animal Center.

Modeling

The rabbits were fixed, anesthetized *via* injection of chloral hydrate at the ear edge, and sacrificed at the corresponding time points. Then, the skin was cut open, and the tibia was cut off and cryopreserved at -80°C for use. The tibia was cut off only in group A. In group B, the antibiotic (an appropriate dose of penicillin sodium) was intramuscularly injected for anti-infective therapy for 5 d (twice a day). In group C, 5 μL of miR-21 siRNA was locally injected for 7 d. At 1-20 d after modeling, the bone tissues, time of bony callus formation, and fracture healing in the three groups were observed by imaging.

Determination of Content of Serum Collagen I and Collagen II

Firstly, 10 mL of blood was drawn from rabbits before and after modeling, respectively. The collected serum samples were separated *via* centrifugation at 2000 rpm for 15 min. Then, these samples were placed at room temperature and stored at -20°C for later use. Subsequently, the cryopreserved serum samples were taken out, followed by detection of the content of serum collagen I and collagen II in the three groups *via* enzyme-linked immunosorbent assay (ELISA, Novus, Littleton, CO, USA).

Reverse Transcription-Polymerase Chain Reaction (RT-PCR)

Absorbance values of RT-PCR amplification products were measured using Image Plus software. Bone tissues of rabbits were added with 1 mL of TRIzol (Invitrogen, Carlsbad, CA, USA) reagent, 0.2 μL of Taq enzyme, 8.3 μL of ddH_2O, and 12.5 μL of 2× Buffer to extract the total RNA. Then, the cells were placed into 5 μL Eppendorf (EP; Hamburg, Germany) tubes. Extracted RNA was reversely transcribed using the A3500 reverse transcription kit. Next, 2 μL of reverse transcription products were stained with nucleic acid gel stain to detect the expressions of the target genes using CFX-96 RT-PCR instrument. The primers used in this study were designed by Sangon (Shanghai, China) (shown in Table I). Specific amplification conditions were as follows: 98°C for 5 min, 10°C for 45 s, 75°C for 30 s, and 80°C for 4 min, for a total of 30 cycles.

Table I. Primer and primer sequences in PCR.

Gene	Primer	Sequence
TGF-β1	Forward	5'-ATGGAGCTGGTGAAACGGAAG-3'
	Reverse	5'-GACTGGCGAGCCTTTGGAC-3'
Smad	Forward	5'-ATGTCGTCATCTTGCCATTC-3'
	Reverse	5'-AACCGTCCTGTTTTCTTTAGCTT-3'
ERK	Forward	5'-TGTTGCCATCAACGACCCCTT-3'
	Reverse	5'-CTCCACGACATACTCAGCA-3'
GAPDH	Forward	5'-TGTTGCCATCAACGACCCCTT-3'
	Reverse	5'-CTCCACGACACATCTCAGCA-3'

Western Blotting

The total protein was first extracted in the tissues, and the concentration of the protein was determined using the bicinchoninic acid (BCA) method (Pierce, Rockford, IL, USA). The protein samples were separated by electrophoresis and transferred onto membranes according to the criteria. Subsequently, the membranes were incubated with primary antibodies of ERK, TGF-β1, and Smad at 4°C overnight. On the next day, the membranes were incubated with corresponding secondary antibodies in the dark at room temperature for 1 h. The immunoreactive bands were finally scanned with Odyssey far-infrared system and analyzed using QuantityOne software.

Histological Observation

Section preparation is described as follows. Firstly, about 2 cm tissue blocks were taken at the fracture end using a sharp knife, soaked in 10% polyformaldehyde solution at 4°C, and fixed for 2 d. Secondly, the tissue blocks were decalcified with ethylene diamine tetraacetic acid (EDTA) for 10 d. Thirdly, the tissue blocks were then soaked in xylene solution and absolute ethanol for 5 min, and stained with hematoxylin for 3 min. After rinsing with distilled water for 3 min and differentiating with differentiation buffer for 30 s, the tissue blocks were dehydrated with gradient ethanol, followed by color separation and sealing with gum. Finally, the sections were observed under a microscope (×400).

Statistical Analysis

The Statistical Product and Service Solutions (SPSS) 15.0 (SPSS, Chicago, IL, USA) software was used for all statistical analysis. The *t*-test was used to compare the differences between the two groups. The analysis of variance was adopted for pairwise comparison within the group, followed by the post-hoc test (Least Significant Difference). Enumeration data were expressed as mean ± standard deviation ($\overline{\chi}$±s). $p<0.05$ was considered statistically significant.

Results

Time of Bony Callus Formation and Fracture Healing

According to the curves at 1, 5, 10, 15, and 20 d, no bony callus formation was observed in group A. Compared with group A, there was bony callus formation in group B. However, the formation rate was relatively low, delaying bone healing. Compared with group B, bony callus formation was significantly improved in group C, and the time of bone healing was remarkably shortened ($p<0.05$) (Figure 1).

Results of Histological Observation

According to the results of HE staining and Masson staining, compared with group A, group C had more fibrous calluses, new capillaries, and fibroblasts in tissues. Meanwhile, there was bet-

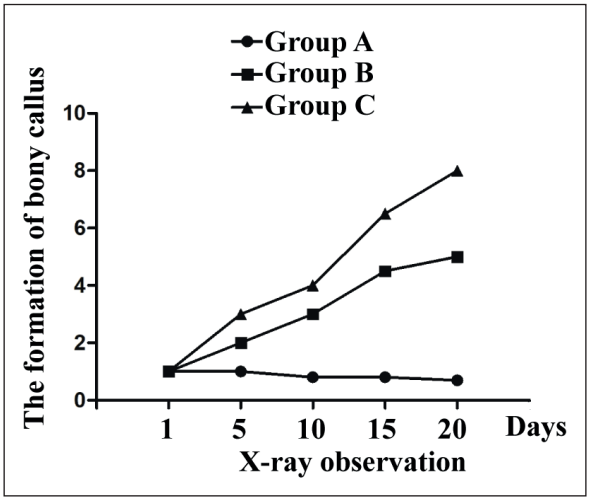

Figure 1. Time of bony callus formation and fracture healing in rabbits. Note: At 1 d, group A, group B, and group C have no bony callus formation without different manifestations. At 5 d, the bony callus formation is greater in group C than that in group A and group B. Meanwhile, it is also greater in group B than that in group A. However, the formation rate is relatively low. At 20 d, bony callus formation reaches the peak in group C, and there are statistically significant differences ($p<0.05$).

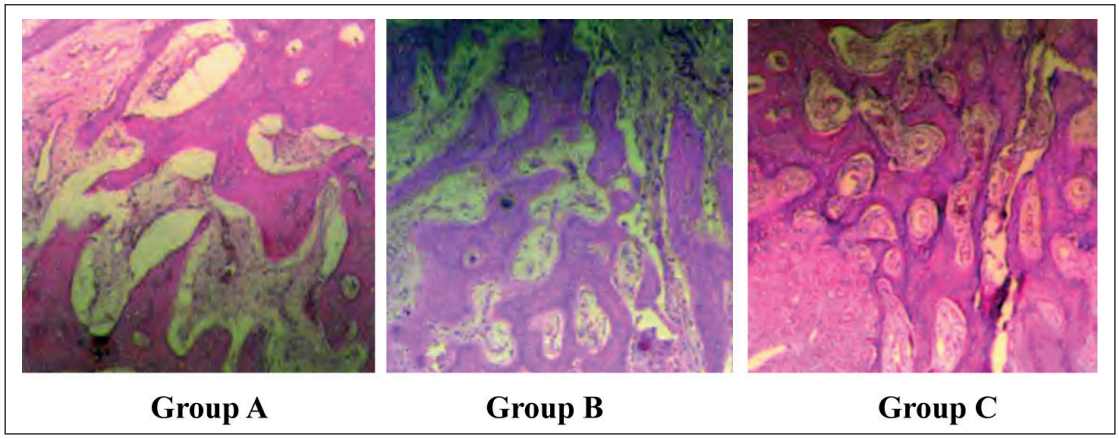

Figure 2. Pathological features of bone healing in each group detected *via* HE staining (×400).

ter maturity of collagen tissues, as well as higher osteoid content at 20 d after modeling in group C. Compared with group C, there were more osteoid tissues with poor maturity in group B. Furthermore, intramembranous bone formation was deformed, and the collagen content was low in group B ($p<0.05$) (Figures 2 and 3).

Content of Serum Collagen I and Collagen II Detected Via ELISA

At 20 d after fracture modeling, the content of the serum collagen I and collagen II significantly increased in group B when compared with group A ($p<0.05$). However, it significantly increased in group C when compared with group B, showing statistically significant differences ($p<0.05$) (Table II).

Protein Content in Osteoblasts Detected Via Western Blotting

Western blotting results demonstrated that the protein expressions of TGF-β1, Smad, and ERK in osteoblasts were remarkably elevated in group B compared with those in group A ($p<0.05$). However, they were significantly higher in group C than those of group B ($p<0.05$) (Figure 4).

RT-PCR Results

RT-PCR results revealed that the messenger RNA (mRNA) expressions of TGF-β1, Smad, and ERK in osteoblasts were remarkably upregulated in group B when compared with group A ($p<0.05$). Moreover, they were also significantly higher in group C than those of group B ($p<0.05$) (Figure 5).

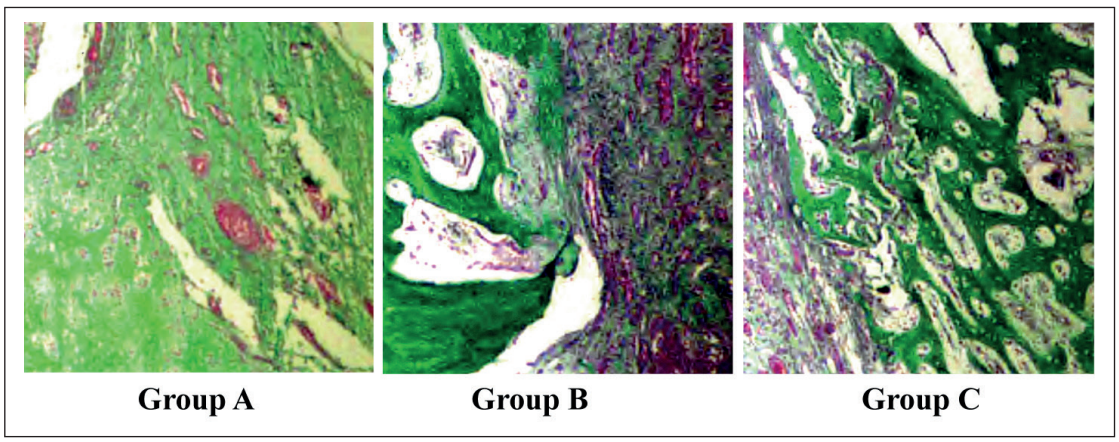

Figure 3. Pathological features of bone healing in each group detected *via* Masson staining (×400).

Table II. Comparison of content of serum collagen I and collagen II in rabbits among groups.

Group	Collagen I	Collagen II
Group A	5.435 ± 2	4.316 ± 1.5
Group B	15.827 ± 6*[1]	12.931 ± 4*[1]
Group C	20.523 ± 4*[2]	21.726 ± 5*[2]

Discussion

Over the past years, the process of fracture healing has been widely studied. Meanwhile, more direct and effective therapeutic regimens have been explored[11]. X-ray film shows that the fracture is accompanied by pain, swelling, and function obstruction, and the bony crepitus is produced. Fracture healing can be divided into three stages, namely hematoma inflammation, bony callus formation, and bone lamella modeling[12]. Bone healing is classified into direct healing and indirect healing. The former refers to natural healing without the influence of external force, while the latter refers to the healing achieved by treatment means[13]. Eliminating hematoma inflammation and promoting bony callus formation are of vital importance throughout the whole process of fracture healing. Vascular wall becomes thickened due to the deposition of bone tissues under inflammatory stimuli and proliferation of fibrotic cells. This may also affect its transformation into osteoblasts[14]. Only by effectively regulating external factors the inflammation can be eliminated. Moreover, the proliferation of bone cells can be promoted, and bony callus formation can be accelerated[15]. Multiple growth factors play important roles during fracture healing, such as insulin-like factors, endothelial cytokines, platelet factors, and other growth factors. They can activate the synthesis of fibrocytes in bone tissues and increase collagen fiber content. Therefore, fibrocytes and intercellular substance are transformed into connective tissues, eventually promoting bone healing[6]. Moreover, some factors promote cell synthesis and differentiation throughout fracture healing. Among them, TGF-β1 has been found to play the most prominent role. Current studies[4] have demonstrated that miR-21 is associated with TGF-β1 and transmitted through the expression of ERK signals. Li et al[15] have indicated that the upregulation of the expression of high-mobility group box 1 under hypoxic conditions can facilitate osteoblast proliferation. The possible underlying mechanism may be related to the activation of the ERK/JNK signaling pathway.

In the current research, the tibial fracture model was first established in rabbits. At 1-20 d, no bony callus formation was observed in group A. Compared with group A, there was bony callus formation in group B. However, the formation rate was relatively low, delaying bone healing. In comparison with group B, bony callus formation was significantly improved, and the time of bone healing was shortened in group C. HE staining and Masson staining indicated that compared with group A, group B had more osteoid tissues with poor maturity and deformed intramembranous osteogenesis at 20 d after modeling. Compared with group B, there were more collagens, fibrous calluses, new capillaries, and fibroblasts in group C. In addition, the time of bony callus formation and healing was significantly longer in group B than those in group A. The content of collagens

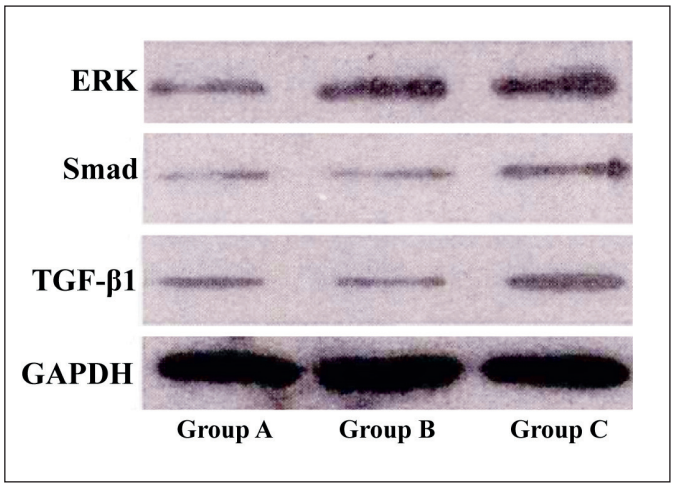

Figure 4. TGF-β1, Smad, and ERK expressions in osteoblasts in rabbits detected *via* Western blotting.

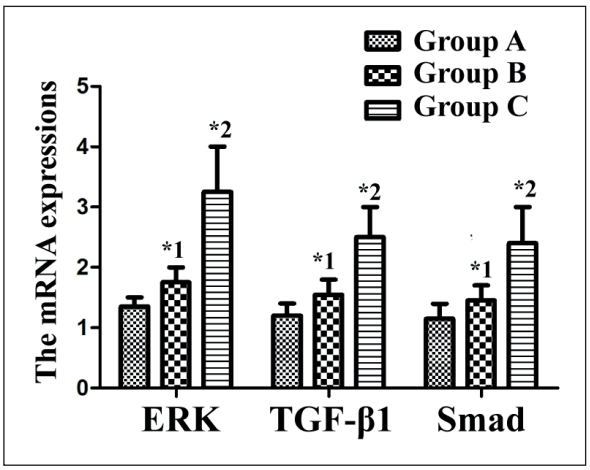

Figure 5. TGF-β1, Smad, and ERK mRNA expressions in osteoblasts in rabbits detected via RT-PCR. Note: *1: $p<0.05$ *vs.* group A, and *2: $p<0.05$ *vs.* group B.

and fibroblasts in tissues was higher in group B. Group C exhibited remarkably more new calluses, higher formation rate and prominently more fibrous connective tissues, collagens, and new capillaries among bone defects than group B. The above findings indicated that the external factor miR-21 could directly or indirectly affect the time of the original bony callus formation in fracture healing[16]. The possible reason was that miR-21 activated a certain protein signal during bone healing. Ultimately, this promoted the proliferation of bone cells, provided required collagens and fibrous connective tissues, and stimulated rapid a formation of bony calluses[17]. The main reason for the shortened time of bony callus formation might be that ERK and downstream target genes at the fracture site were activated to accelerate bone healing[18]. To sum up, the downregulation of miR-21 promoted bone healing by upregulating the downstream target genes of the ERK signaling pathway.

Activating the expression of growth factors affects fracture healing state. This can regulate osteoblast differentiation, increase collagen content, and osteoblast proliferation rate, as well as produce new bone matrixes to some extent[19]. The content of serum collagen I and collagen II was detected *via* ELISA in this study. The results showed that the content of serum collagen I and collagen II significantly increased in group B when compared with that in group A. However, it was persistently raised in group C in comparison with group B. Western blotting results demonstrated that the protein expressions of TGF-β1, Smad, and ERK were significantly higher in group B when compared with those in group A ($p<0.05$). However, they were remarkably elevated in group C when compared with group B, showing statistically significant differences ($p<0.05$). RT-PCR results revealed that the mRNA expressions of TGF-β1, Smad, and ERK in osteoblasts remarkably increased in group B in comparison with group A ($p<0.05$). However, they were significantly elevated in group C when compared with group B ($p<0.05$). The above results demonstrated that inhibiting miR-21 expression could not only promote osteoblast differentiation, but also further facilitate new bone mineralization. Besides, suppressing the expression of miR-21 activated the expressions of the downstream proteins TGF-β1 and Smad by regulating the ERK protein, thereby promoting fracture healing. Our findings suggested that there was a positive correlation between the expressions of miR-21 and ERK signals. TGF-β1 and Smad protein expressions increased in the case of high expression of ERK[20,21], however, they were inhibited in the case of low expression of ERK.

Conclusions

We first found that the downregulation of miR-21 promotes osteoblast proliferation, increases bone collagen formation, shortens the prime time for bone healing and accelerates the new bone formation and mineralization by positively regulating the expressions of the downstream growth factors in ERK signal transduction pathway.

Conflict of Interests

The authors declared that they have no conflict of interests.

References

1) Liu CH, Huang Q, Jin ZY, Zhu CL, Liu Z, Wang C. MiR-21 and KLF4 jointly augment epithelialmesenchymal transition via the Akt/ERK1/2 pathway. Int J Oncol 2017; 50: 1109-1115.
2) Yang P, Sun D, Jiang F. Ailanthone promotes human vestibular schwannoma cell apoptosis and autophagy by downregulation of miR-21. Oncol Res 2018; 26: 941-948.
3) Sun NN, Yu CH, Pan MX, Zhang Y, Zheng BJ, Yang QJ, Zheng ZM, Meng Y. Mir-21 mediates the inhibitory effect of Ang (1-7) on AngII-induced NLRP3 inflammasome activation by targeting Spry1 in lung fibroblasts. Sci Rep 2017; 7: 14369.

4) Friedman A, Hao W. Mathematical modeling of liver fibrosis. Math Biosci Eng 2017; 14: 143-164.
5) Huang X, Yue Z, Wu J, Chen J, Wang S, Wu J, Ren L, Zhang A, Deng P, Wang K, Wu C, Ding X, Ye P, Xia J. MicroRNA-21 knockout exacerbates angiotensin II-induced thoracic aortic aneurysm and dissection in mice with abnormal transforming growth factor-beta-SMAD3 signaling. Arterioscler Thromb Vasc Biol 2018; 38: 1086-1101.
6) Haque R, Iuvone PM, He L, Choi K, Ngo A, Gokhale S, Aseem M, Park D. The microRNA-21 signaling pathway is involved in prorenin receptor (PRR)-induced VEGF expression in ARPE-19 cells under a hyperglycemic condition. Mol Vis 2017; 23: 251-262.
7) Masoudi MS, Mehrabian E, Mirzaei H. MiR-21: a key player in glioblastoma pathogenesis. J Cell Biochem 2018; 119: 1285-1290.
8) Wang YX, Zhao JR, Xu YY, Wu WB, Zhang HJ. MiR-21 is overexpressed in hydatidiform mole tissues and promotes proliferation, migration, and invasion in choriocarcinoma cells. Int J Gynecol Cancer 2017; 27: 364-374.
9) Wang GB, Liu JH, Hu J, Xue K. MiR-21 enhanced glioma cells resistance to carmustine via decreasing Spry2 expression. Eur Rev Med Pharmacol Sci 2017; 21: 5065-5071.
10) Kanokudom S, Vilaivan T, Wikan N, Thepparit C, Smith DR, Assavalapsakul W. MiR-21 promotes dengue virus serotype 2 replication in HepG2 cells. Antiviral Res 2017; 142: 169-177.
11) Zhao MY, Wang LM, Liu J, Huang X, Liu J, Zhang YF. MiR-21 suppresses Anoikis through targeting PDCD4 and PTEN in human esophageal adenocarcinoma. Curr Med Sci 2018; 38: 245-251.
12) Long S, Zhao N, Ge L, Wang G, Ran X, Wang J, Su Y, Wang T. MiR-21 ameliorates age-associated skin wound healing defects in mice. J Gene Med 2018; 20: e3022.
13) Liu CH, Huang Q, Jin ZY, Zhu CL, Liu Z, Wang C. MiR-21 and KLF4 jointly augment epithelialmesenchymal transition via the Akt/ERK1/2 pathway. Int J Oncol 2017; 50: 1109-1115.
14) Ning ZW, Luo XY, Wang GZ, Li Y, Pan MX, Yang RQ, Ling XG, Huang S, Ma XX, Jin SY, Wang D, Li X. MicroRNA-21 mediates Angiotensin II-induced liver fibrosis by activating NLRP3 inflammasome/IL-1beta axis via targeting Smad7 and Spry1. Antioxid Redox Signal 2017; 27: 1-20.
15) Li Q, Yu B, Yang P. Hypoxia-induced HMGB1 in would tissues promotes the osteoblast cell proliferation via activating ERK/JNK signaling. Int J Clin Exp Med 2015; 8: 15087-15097.
16) Yang YZ, Zhang XY, Wan Q, Li J. [Role of exosomal miRNA in multiple myeloma progression and its possible mechanism-review]. Zhongguo Shi Yan Xue Ye Xue Za Zhi 2017; 25: 301-305.
17) Yang S, Dong F, Li D, Sun H, Wu B, Sun T, Wang Y, Shen P, Ji F, Zhou D. Persistent distention of colon damages interstitial cells of Cajal through Ca(2+)-ERK-AP-1-miR-34c-SCF deregulation. J Cell Mol Med 2017; 21: 1881-1892.
18) Eyvazi S, Kazemi B, Dastmalchi S, Bandehpour M. Involvement of CD24 in multiple cancer related pathways makes it an interesting new target for cancer therapy. Curr Cancer Drug Targets 2018; 18: 328-336.
19) Li ZH, Li L, Kang LP, Wang Y. MicroRNA-92a promotes tumor growth and suppresses immune function through activation of MAPK/ERK signaling pathway by inhibiting PTEN in mice bearing U14 cervical cancer. Cancer Med 2018. doi: 10.1002/cam4.1329. [Epub ahead of print].
20) Alles J, Ludwig N, Rheinheimer S, Leidinger P, Grasser FA, Keller A, Meese E. MiR-148a impairs Ras/ERK signaling in B lymphocytes by targeting SOS proteins. Oncotarget 2017; 8: 56417-56427.
21) Gui ZL, Wu TL, Zhao GC, Lin ZX, Xu HG. MicroRNA-497 suppress osteosarcoma by targeting MAPK/Erk pathway. Bratisl Lek Listy 2017; 118: 449-452.